Title
Physiological activation and deactivation of soluble guanylate cyclase

Authors
Horst, Benjamin G
Marletta, Michael A

Publication Date
2018-07-01

DOI
10.1016/j.niox.2018.04.011

Peer reviewed

Published in final edited form as:

Nitric Oxide. 2018 July 01; 77: 65–74. doi:10.1016/j.niox.2018.04.011.

Physiological activation and deactivation of soluble guanylate cyclase

Benjamin G. Horst[a], **Michael A. Marletta**[a,b,c,*]

[a]Department of Chemistry, University of California, Berkeley, Berkeley, CA, USA

[b]Department of Molecular and Cell Biology, University of California, Berkeley, Berkeley, CA, USA

[c]California Institute for Quantitative Biosciences, University of California, Berkeley, Berkeley, CA, USA

Abstract

Soluble guanylate cyclase (sGC) is responsible for transducing the gaseous signaling molecule nitric oxide (NO) into the ubiquitous secondary signaling messenger cyclic guanosine monophosphate in eukaryotic organisms. sGC is exquisitely tuned to respond to low levels of NO, allowing cells to respond to non-toxic levels of NO. In this review, the structure of sGC is discussed in the context of sGC activation and deactivation. The sequence of events in the activation pathway are described into a comprehensive model of *in vivo* sGC activation as elucidated both from studies with purified enzyme and those done in cells. This model is then used to discuss the deactivation of sGC, as well as the molecular mechanisms of pathophysiological deactivation.

Keywords

Soluble guanylate cyclase; Nitric oxide; Heme cofactor; Allosteric activation

1. Introduction

In the 1980s, nitric oxide (NO) was first characterized as critical to both innate immunity and endogenous signaling in animals [1–5]. NO was the first gaseous signaling molecule synthesized by animals to have its biochemical signaling pathway fully described [2]. Physiologically, NO signaling causes relaxation of vascular smooth muscle, inhibition of platelet aggregation in the vasculature, and modulation of various forms of neurotransmission [6,7]. Beyond these well-established functions, additional aspects of NO signaling continue to emerge, including in insect development and sensory systems [8], as well as in human pathologies, such as early-onset achalasia [9] and cancer proliferation [10].

*Corresponding author. Department of Chemistry, University of California, Berkeley, Berkeley, CA, USA. marletta@berkeley.edu (M.A. Marletta).

Conflicts of interest

The authors declare no competing financial interests.

Appendix A. Supplementary data

Supplementary data related to this article can be found at http://dx.doi.org/10.1016/j.niox.2018.04.011.

Soluble guanylate cyclase (sGC), a eukaryotic nitric oxide receptor, is a central component in NO−dependent signaling [3,11]. sGC converts 5'-guanosine triphosphate (GTP) to 3',5'-cyclic guanosine monophosphate (cGMP). When NO binds to sGC, enzyme activity increases several hundredfold, transducing the gaseous paracrine-signaling molecule to a ubiquitous secondary signaling molecule. The molecular details of how NO activates sGC to maximal physiological activity are not fully understood, though much progress has been made.

Aberrations resulting in decreased function of this sGC-dependent signaling pathway have been linked to multiple pathologies, including cardiovascular disease, hypertension, asthma, and neurodegeneration [12,13]. Many emergent pharmaceuticals seek to increase sGC activity in these diseased states. One set of examples are the sGC stimulators, initially exemplified by the benzylindazol compound YC-1 [14] and culminating in Bayer's riociguat (Adempas*), the latter was approved by the FDA in – to treat pulmonary arterial hypertension and chronic thromboembolic pulmonary hypertension [15]. This class of molecules has also added to our understanding of the NO−dependent activation mechanism of sGC, however it is still unclear how these molecules by themselves promote the active conformation of sGC [16,17].

This review combines structural and functional aspects of NO−dependent activation and deactivation of sGC to build a model of sGC activation *in vivo.* Stimulators and activators are discussed in the context of physiological activation, and interested readers are directed to other reviews [17,18] that are dedicated to these small molecules.

2 Structure of soluble guanylate cyclase

Soluble guanylate cyclase is a heterodimer comprised of an α and a β subunit (Fig. 1A). Multiple isoforms of these two subunits have been identified, yet sGC is most commonly expressed as a heterodimer composed of α_1 and β_1 subunits (Uniprot IDs of *Homo sapiens* α_1 and β_1 proteins: Q02108 and Q02153) [19]. Each subunit consists of four domains: a heme nitric oxide and oxygen binding (H−NOX) domain [20], a Per-Arnt-Sim (PAS)-like domain, a coiled-coil (CC) domain, and one subunit of the catalytic heterodimer (CAT). Although the H−NOX subunit structures are similar, only the β subunit has the capacity to bind heme. Since a high-resolution structure of full-length sGC has yet to be obtained, the vast majority of structural information is derived from isolated domains of sGCs. Others have recently reviewed the structure of sGC [21,22], and thus the discussion here will be limited to pertinent details and recent developments.

H−NOX domains, also known as heme nitric oxide binding (HNOB) or sensor of nitric oxide (SONO) domains [23], consist of an N-terminal alpha helical subdomain and a C-terminal subdomain composed of alpha helices and four antiparallel beta sheets. A single heme cofactor binds in a central cavity between the two subdomains (Fig. 1B). The N-terminal and C-terminal subdomains are termed distal and proximal, respectively, with the proximal subdomain defined by the presence of a heme-ligating histidine residue (termed the proximal histidine). H−NOX domains are also found as stand-alone proteins in prokaryotes [24], and the study of these proteins has greatly improved our understanding of how these

domains bind gaseous ligands and transduce chemical signals [25–28]. These studies, as well as spectroscopic studies of sGC, showed that NO initially binds to the 5-coordinate (5c) high-spin ferrous heme cofactor (5c His−$Fe2^{+)}$, which leads to a transient 6-coordinate (6c) complex (6c His−$Fe2^{+}$−NO) [29–31]. This complex, driven by the strong σ trans effect NO exerts on the proximal histidine, spontaneously dissociates to the 5c low-spin ferrous nitrosyl complex (5c Fe^{2+}−NO) [32]. In turn, cleavage of the iron-histidine bond results in a 90° rotation of the α-helix (α F) that contains the histidine; this conformational change is thought to be the initial step in propagating the NO signal [33]. Some studies have examined the next steps in signal transduction pathway by examining other residues on the α F helix, however, it remains unclear exactly how these events confer full activity to the enzyme [34,35].

The PAS and CC domains of sGC have been studied less by comparison, though their function in sGC signal transduction is likely important. PAS domains are versatile as they can play varied roles in different proteins, such as quaternary structure organization, cofactor binding, and signal transduction [36–38]. Indeed, in sGC the PAS domains are implicated in dimerization [39], gas binding [40], and Hsp90-mediated heme insertion [41]. Additionally, the crystal structure of the *Manduca sexta* sGC α_1 PAS domain was recently solved, revealing an extra beta strand and a flexible helix that could be important for transducing the NO signal [42]; however, the exact mechanism of signal transduction is still not fully understood. The first crystal structure of the β CC domain in sGC exhibited the coils oriented in an anti-parallel orientation [43]. More recently, cross-linking mass spectrometry and single particle electron microscopy experiments suggest that the orientation of these helices are parallel in the native structure [40,44]. Through the use of hydrogen deuterium exchange mass spectrometry, the linker region between the PAS and the CC domains has been shown to undergo remarkable solvent exchange dynamics with the addition of NO, suggesting that conformational changes affect this linker region in an NO−dependent manner [45]. Since the PAS/CC linker region appears to be important for transducing the NO signal, additional studies to elucidate the molecular details of this process will be very important.

The CAT domains of sGC are members of the Class III nucleotide cyclase domain family, as determined by sequence analysis and secondary structural motifs [46–49]. The CAT domains form a heterodimer: one active site and one pseudosymmetric site are formed at the interface of the a and p subunits. ATP is a mixed-type inhibitor of sGC and this pseudosymmetric site is proposed to be the site of ATP action [16,50,51]. The interested reader is directed to the review in this issue by Childers et al. for more details on the structure and function of the CAT domain.

A full-length crystal structure of sGC has yet to be obtained, likely due to conformational flexibility in the quaternary structure in conjunction with challenges of expressing sufficiently large quantities. However, Campbell et al. [44] successfully used single particle electron microscopy to visualize the quaternary structure of sGC. The H−NOX and PAS domains were clustered in a heterotetramer-like lobe at one end of the particle, while the CAT domains formed a tight heterodimeric lobe on the opposing end with the CC domain forming a bridge (Fig. 2). These studies showed that sGC is highly flexible in the presence

and absence of NO, independent of the pH of the stain. Recently, Vercellino et al. [52] solved the first crystal structure containing both the CC and the CAT domains of an adenylate cyclase from *Mycobacterium intracellulare*. Because these structural motifs are conserved across many nucleotidyl cyclases, this crystal structure can be used to improve modeling of the quaternary structure of sGC, as shown in Fig. 2.

There are two hypotheses that predict how the quaternary structure of sGC changes upon NO activation. It has been postulated that the β H−NOX domain comes in direct contact with the α CAT domain through space to inhibit CAT domain activity (Fig. 3A). Alternatively, it has been proposed that the signal transduction event occurs through the protein backbone (Fig. 3B). The hypothesis that the β H−NOX domain directly inhibits the catalytic activity is based on individual H−NOX domain inhibition of catalytic activity *in trans*, and cross-linking experiments establishing contacts between these two domains [40,53]. Support for the signal transduction event to take place through the protein backbone comes from the observation of NO−independent flexibility observed by electron microscopy [44]. While it is possible that some continuum between these two extremes is physiologically relevant, what, if any, conformational change occurs in sGC during signal transduction remains an outstanding question in the field.

3. Activation of soluble guanylate cyclase

The molecular steps involved in sGC activation have evolved significantly over the last several years. The key studies are outlined below, but here we provide an overall summary. The activation mechanism of sGC was initially proposed to be relatively simple, where the 5c Fe^{2+}−NO heme complex generated upon NO binding led to fully active enzyme. Detailed kinetic studies on NO binding to the heme and enzyme activity has led to a more complicated mechanism, perhaps in hindsight not unexpected given the pivotal role played by sGC in human physiology. There are two aspects to NO activation of sGC. The first involves the formation the 5c ferrous nitrosyl heme complex, and the most recent evidence is consistent with a distal version of this species (5c Fe^{2+}−NO). sGC treated with 1 equivalent of NO is activated to only ~15% of maximal activity. Addition of excess NO fully activates sGC *and* increases the rate at which the 5c Fe^{2+}−NO heme complex forms from the 6c His −Fe^{2+}−NO species. All evidence points towards a second NO binding site for the action of this excess NO as discussed below.

3.1. NO binding to the H−NOX domain

It is well established that the first step in sGC activation is NO binding to the 5c His−Fe2+ heme cofactor in the β1 H−NOX domain [29–31]. The resulting 6c His− Fe^{2+}−NO complex has been observed by stopped-flow UV-Vis spectroscopy and electron paramagnetic resonance (EPR) spectroscopy with samples prepared at 4 °C or lower to slow iron–histidyl bond scission [29,54–57]. The strong 0 trans effect of NO ruptures the iron–histidyl bond ($k_{6c} \rightarrow k_{5c} = 50{,}000 M^{-1}s^{-1}$), resulting in a 5c Fe^{2+}−NO heme complex, which exhibits a relatively long half-life in solution (k_{off} for NO = 0.0006 s^{-1}) compared to other species in sGC activation (discussed below) [30,58]. Even so, it was only recently that Herzik et al. solved a crystal structure of the 5c ferrous nitrosyl H−NOX domain, using the H−NOX

protein from the gamma proteobacterium *Shewanella oneidensis (So)* [33]. This study also used a stable 6c His−Mn^{2+}−NO porphyrin complex to characterize possible structural changes in the H−NOX domain due to gas binding, removing the complication of iron–histidyl bond cleavage [59]. The root mean square deviation of the atoms in the 5c His −Mn^{2+} structure aligned to the 6c His−Mn^{2+}−NO structure was 0.099 Å, indicating that the driving force behind iron–histidyl bond cleavage is the 0 trans effect of NO rather than any structural rearrangement resulting from ligand binding. These results support the hypothesis that the H−NOX conformational change is dependent on iron–histidyl bond cleavage [29,59].

Two hypotheses have been proposed for H−NOX conformational change required to initiate a gas-induced activity change in a response regulator. Ma et al. solved crystal structures of the unliganded, NO−bound, and CO-bound H−NOX protein from *Nostoc* sp., and found that in this H−NOX, both ligands formed 6c complexes. The authors proposed a heme pivoting mechanism that is dependent on gas binding for signal transduction. Herzik et al. compared the structures of *Shewanella oneidensis* with and without NO and described a relative motion of the N-terminal and C-terminal subdomains along a pair of conserved glycines, termed the “glycine hinge” (Fig. 1B). However, the mechanism of H−NOX induced conformational change resulting in activation of sGC is currently not known, and await high resolution structures of full-length sGC with and without NO bound for clarification of these possibilities.

3.2. Connecting NO binding to iron–histidyl bond cleavage

Stone et al. [54] first observed an unexpected phenomenon that indicated interaction of NO with sGC is not as simple as NO binding to the heme: the rate of conversion of 6c His−$Fe2^{+}$ −NO to 5c Fe^{2+}−NO depends on the concentration of NO. This result was then expanded upon by Zhao et al. (Fig. 4) [29]. This surprising concentration dependence implies that a second molecule of NO must interact with the 6c His−$Fe2^{+}$−NO sGC enzyme to influence the rate of iron–histidyl bond dissociation. There are several proposals for this additional interaction: a second, non-heme NO binding site that could be covalent or non-covalent; nucleophilic addition of NO to the heme-bound NO; or a second NO binding to the proximal side of the heme. These proposals remain somewhat contested [60,61], and the molecular basis for this concentration dependence has yet to be conclusively demonstrated. Given that two of the proposals are difficult to test experimentally, namely nucleophilic addition of NO to the heme-bound NO and a hydrophobic site specific for NO, in this section we review the major studies that seek to determine whether this dependence on NO concentration of histidine dissociation is due to a second NO binding event on the proximal side of the heme. The next section of the review will be devoted to articles focused on a second non-heme NO binding site.

When the hypothesis that NO could bind to the proximal side of the heme was first proposed in 1999 by Zhao et al. [29], cleavage of the iron–histidyl bond was considered to be the only step necessary to fully activate sGC. NO first must bind to the distal side of the heme forming a transient 6c His−Fe^{2+}−NO complex before iron-histidine bond cleavage leading to 5c Fe^{2+}−NO (Fig. 5A, species (1) → (2) → (3)). Accordingly, the re-formation of the iron–

histidyl bond was thought to be the only step involved in sGC deactivation. When NO binds to the distal face of the heme (5c Fe^{2+}−NO), the dissociation path is straightforward. By the principle of microscopic reversibility, NO would dissociate in the reverse path of its association (Fig. 5A, species (3) → (2) → (1)). However, if NO binds to the proximal face of the heme (5c NO−Fe^{2+}), it is not clear how NO would dissociate, assuming the generation of a 4-coordinate porphyrin is energetically unfeasible (not depicted) (Fig. 5B, (5) → (1)). Without excess NO (or another ligand) to bind and reform a 6c species, the dissociation of proximal NO would not be easily reversed.

Nonetheless, several studies have found NO bound in the proximal pocket of bacterial H−NOX proteins and in the H−NOX domain of sGC. In the NO−bound crystal structure of *So* H−NOX mentioned above, electron density corresponding to the NO ligand was observed on the proximal side of the heme (5c NO−Fe^{2+}). In this structure with the proximal ligation of NO, the proximal histidine was shifted 8.5 Å and the αF helix rotated 90° (Fig. 1B). Proximal NO ligation was also observed in an earlier crystal structure of cytochrome c' from *Alcaligenes xylosoxidans.* Although the protein structures are unrelated, this cytochrome c', also forms a 5c NO−Fe^{2+} heme cofactor via a 6c dinitrosyl complex (6c NO−Fe^{2+}−NO) [62]. However, the crystal structure of the *So* H−NOX domain provided the first crystallographic evidence that NO can bind to the proximal side of the heme in H−NOX domains, and thus potentially in sGC. The structure of the 5c NO−Fe^{2+} H−NOX exhibited a displacement of the distal domain by 2.5 Å compared to the 5c His−$Fe2^{+}$ structure, when the two structures were aligned by the proximal domain (Fig. 1B). A similar displacement was also observed in prokaryotic O_2-sensing H−NOX domains, suggesting that these structural changes upon gas binding may be universal for the signal transduction of gases through H−NOX domains, including in sGC [63].

In 2012, Martin et al. [56] found that NO could coordinate to the proximal side of the heme in full-length sGC. Rapid freeze quench (RFQ) EPR with isotopically labeled NO was used to discern which isotopes of NO bound to the heme under sequential mixing conditions. First, 5c His−$Fe2^{+}$ sGC was mixed with ^{14}NO to generate 6c His−Fe^{2+}–^{14}NO, then ^{15}NO was added and the samples were rapidly frozen after approximately 5 s. Isotopically mixed 5c samples were measured by EPR, implying the formation of two different populations: ferrous nitrosyl heme with either ^{14}NO or ^{15}NO bound. Although this EPR experiment does not distinguish between NO bound to the distal or the proximal side, the experimental design was such that the NO isotope used in the second addition must initially bind to the proximal side. The authors were able to show that the ratio of ^{14}NO:^{15}NO bound to sGC was influenced by the concentration of ^{15}NO used. For example, whereas an equimolar concentration ratio of ^{14}NO:^{15}NO gave sGC populations with 43:57 (^{14}NO:^{15}NO) bound, ten-fold excess of ^{15}NO led to an sGC population of 15:85 (^{14}NO:^{15}NO). This concentration dependence indicates that on this timescale, NO−Fe^{2+}−NO forms, however it is not clear how many times NO is binding to the heme so NO could be proximal or distal (species (3), (4), and (5) in Fig. 5). Under these conditions on the timescale of milliseconds to seconds, NO is binding to the proximal side of the heme, and the authors conclude that the proximal side of the heme is the site where the second NO molecule binds.

Conversely, Yoo et al. [30] studied the motion of the proximal histidine of sGC with NO present by using time-resolved absorption spectroscopy on timescales from nanoseconds to milliseconds, and did not see evidence of NO binding to the proximal side of the heme. Previous work by the authors established that laser flash photolysis of ferrous nitrosyl heme to generate the 4c Fe^{2+} species resulted in 97% geminately recombined ferrous nitrosyl heme (τ = 7.5 ps) [64,65]. They then examined the 3% of heme that did not geminately recombine with NO; this population rebound the proximal histidine to form 5c His−Fe^{2+} (τ_0 = 70 ps). Following this 5c His−Fe^{2+} species, four specific transitions were identified spanning nanosecond to millisecond timescales (Fig. 6). Of these, the first two spectral changes to occur were unaffected by NO concentration: 6c His−Fe^{2+}−NO formation (τ_1 = 6.5 ns), and the subsequent iron–histidyl bond scission to form 5c Fe^{2+}−NO (τ_2 = 0.66 is). These early events were attributed to geminate recombination of NO to the heme after the laser pulse has ended, and subsequent iron–histidyl bond rupture. The spectral changes resulting from geminate recombination of NO ($\tau_1$and τ_2) are an outcome of the experimental setup where the initial condition of ferrous nitrosyl sGC is followed by NO dissociation from the heme. Additional processes occur on longer timescales and are dependent on NO concentration: 6c His−Fe^{2+}−NO formation (τ_3) and iron–histidyl bond scission (τ_4). Concentrations of 20 μM and 200 μM were used, bracketing the lifetimes of these processes at 50 μs ≤ τ_3 ≤ 250 is and 10 ms ≤ τ_4 ≤ 43 ms, which are consistent with bimolecular rates measured by stopped-flow UV-Visible spectroscopy [29]. The authors conclude that these four observed kinetic transitions can be described by a model where NO only binds to the distal side of the heme, at least within a window of 200 ms following initial NO binding.

Importantly, Yoo et al. [30] observed that the slow iron–histidyl bond rupture (τ_4) is NO −dependent, consistent with results from Zhao et al. [29] The transition that is dependent on NO concentration is strictly 6c His−Fe^{2+}−NO to 5c Fe^{2+}−NO. Since no spectral signature of the 6c NO−Fe^{2+}−NO was observed (or any higher Fe^{2+} coordination species as has been postulated), the hypothesis that the NO dependence of the iron–histidyl bond scission is caused by NO binding to the proximal side of the heme is not supported by this data [56]. It is noteworthy that the lifetime of the fast iron–histidyl bond scission (t_2) is independent of NO concentration and is faster than the predicted timescale for protein conformational changes (1–50 is), suggesting there is an additional, unobserved change in sGC that has different effects on the fast and slow iron–histidyl bond dissociation rates. However, for the reasons outlined above, this change cannot be a result of proximal NO binding. It has also been shown that treating sGC with excess NO then rapidly quenching the reaction activates sGC on sub-second time scales, as fast as 200 ms [29]. When evaluated in the context of the time-resolved data, this suggests that bimolecular NO binding and iron–histidyl bond cleavage occurs prior to sGC activation, but before proximal NO formation.

On timescales shorter than a second, it appears that sGC does not form a proximal NO complex. However, such a complex may form under steady-state conditions. One result of this hypothesis would be that the 5c NO−Fe^{2+} species would require excess NO to access 5c Fe^{2+}−NO via a 6-coordinate intermediate (Fig. 5B, species (5) → (3)), and thus would be predicted to dissociate more rapidly with excess NO than with substoichiometric NO. To evaluate whether the proximal NO complex forms under steady-state conditions, Guo et al. [66] measured the NO off-rate for a bacterial H−NOX from *S. oneidensis* under steady-state

conditions with substoichiometric or excess NO. However, the observed off-rates were the same within experimental error and are inconsistent with a model where the primary species in solution is 5c NO−Fe^{2+}. Double electron-electron resonance electron paramagnetic resonance (DEER-EPR) spectroscopy was then used to measure the distance from NO to a spin label bound to a surface cysteine residue located 23 Å from the distal side of the heme and 28 Å from the proximal side of the heme. This experiment enabled the differentiation of NO bound to the proximal and distal sides of the heme. While some proximal NO is observed in the presence of excess NO, the major species was in all cases 5c Fe^{2+}−NO. In fact, when treated with excess NO and then that excess was removed, NO in that case was found only in the distal position.

Given the disparate conclusions from these studies, is it possible to reconcile these differences into a unified model for sGC activation? One hypothesis is that the proximal NO −bound species is more rigid than the distal analog, which enabled the selective crystallization of proximal-bound NO H−NOX. Both the RFQ-EPR and DEER-EPR studies indicate that the proximal NO species can form with sufficient time and NO concentration, however, the primary species at equilibrium is the distal NO complex. If the proximal NO complex were to form, it would occur after the iron–histidyl bond has been broken and sGC has already been activated, given the timescale of these processes. Taken together, it appears that NO binding to the proximal side of the heme is likely not the reason for the NO dependence of iron–histidyl bond scission which, in turn, is necessary but not sufficient for physiological activation of sGC.

3.3. NO binding to the second site of sGC for full physiological activation

Alternative hypotheses exist to explain the NO dependence of the iron–histidyl bond cleavage. Specifically, several groups have postulated that a second, non-heme NO binding site exists elsewhere on sGC. Here, the biochemical evidence for this secondary binding site will be discussed.

The first biochemical evidence for a second NO binding site was characterized by Bellamy et al., in 2002 [67]. The authors measured the activation of sGC using constant or clamped NO concentrations (where the addition of a NO donor is in equilibrium with a NO scavenger) and found that the Hill coefficient of sGC to be 2.1. This suggests that there is cooperativity in the binding of more than one NO molecule to sGC, and the molecular steps in full activation of sGC involve more than NO binding to the heme. In 2004, Russwurm et al. [68] measured both the UV-Vis spectrum and the activity of sGC in the same sample. Upon the addition of excess NO, the UV-Visible spectrum remained unchanged, but the activity increased dramatically compared to substoichiometric amounts of NO. The authors found they could generate a low activity state of sGC by either adding a sub-stoichiometric amount of NO relative to sGC, or by removing excess, non-heme bound NO by a buffer exchange. These results suggested that sGC exists in two different activity states, depending on the concentration of NO, without any changes to the 5c ferrous-nitrosyl heme. The proposed second site has a dissociation constant much higher than that of the heme cofactor ($K_d < 1.2 \times 10^{-12}$M) [29]. The substiochiometric, low-activity state will be henceforth referred to as the 1−NO state, indicating that one NO is bound to sGC at the heme and the

enzyme is in a low activity state. The occupancy of the heme by NO under these conditions is 100%.

In 2005, Cary et al. [16] compared enzymatic activity to the dissociation rate of NO in sGC. The authors found that sGC deactivates over 150 times faster than NO dissociates from the heme with purified enzyme, indicating that NO dissociation does not directly cause sGC deactivation. These results suggest that a binary model of sGC activation and deactivation is likely incomplete. Corroborating Russwurm's data, the authors isolated 1-NO sGC with low activity by using two different traps that bind excess, non-heme bound NO, further indicating that breaking the His−Fe^{2+} bond is not sufficient to fully activate sGC. Additionally, the authors found that YC-1, a known stimulator of sGC activity, fully activates the 1-NO state and has only a small effect on the activity of sGC when excess NO is present. Subsequent deactivation of the 1-NO sGC with YC-1 present occurs slowly. This result is critical to discussing the activation of sGC in cells, discussed below. The model proposed in this paper is a three-activity model of sGC, where sGC has basal activity without NO, ~15% activity with one equivalent of NO, and 100% activity when excess NO is present.

In a slightly different approach, Derbyshire et al. [69] used butyl isocyanate (BIC) as a ferrous distal heme ligand (6c His−Fe^{2+}-BIC) to block diatomic gases from binding to the heme. With BIC as the distal ligand, it was found that the addition of excess NO resulted in a slight shift in the Soret band from 429 nm to 432 nm. This result indicates that excess NO affected the heme environment without replacing the BIC ligand, as ferrous nitrosyl heme would exhibit a Soret band at 399 nm. BIC-bound sGC was activated 5-fold over basal activity in the absence of NO, compared to BIC-bound sGC with excess NO was activated 89-fold over basal. Addition of dithionite, which reacts with all non-heme bound NO, eliminated this additional activity. Together, these findings strongly suggest that there is a second, non-heme NO binding site whose occupancy is required for full sGC activation.

Fernhoff et al. [70] hypothesized that the second NO molecule interacts with a cysteine residue on sGC. In this study, the authors used *S*-methyl methanethiosulfonate (MMTS), a small molecule that reversibly reacts with thiols to form an *S*-methyl-cysteine disulfide bond. When the cysteines of sGC formed a disulfide bond with MMTS, the activity was ~ 15% of maximal activity with excess NO (Fig. 7A) and is nearly identical to the activity of the 1-NO state (Fig. 7D). Under these conditions, all heme was found to be in the ferrous nitrosyl state. Maximal activity was restored upon the addition of excess thiol to remove the MMTS label, thus returning the cysteine disulfides to the native thiol (R-SH) (Fig. 7C). Excess MMTS did not affect the basal activity of sGC (Fig. 7B).

The interaction of thiols and NO is not a new idea. *S*-nitrosation is a known chemical modification of proteins that has been studied for nearly two decades. However, formation of *S*-nitrosothiols (RSNO) requires a one-electron oxidation of NO, and is thus dependent on the presence of an oxidant. Conversely, sGC activation does not dependent on oxidation [70]. Additionally, the half-life of an *S*-nitrosothiol is on the order of hours, which is far longer than the timescale of sGC deactivation which occurs in seconds. Therefore, the authors proposed that NO interacts with an sGC cysteine as a transient *S*-nitrosylthiol radical

anion ($RSNO^{\bullet -}$). While $RSNO^{\bullet -}$ and RNSO differ by only one electron, that single electron dramatically changes the properties of the complex. The half-life of an *S*-nitrosylthiol radical anion could be stabilized by adjacent residues via electrostatic interactions. Additionally, the nucleophilic addition of a thiolate to NO to generate $RSNO^{\bullet -}$ is freely reversible. Such an interaction is commensurate with the concentration of free NO in cells and provides a rapid physiologically-relevant deactivation mechanism of sGC. Since the critical cysteine(s) involved in this transient interaction have yet to be identified, the NO −cysteine interaction remains a hypothesis, albeit with compelling evidence to support it.

An NO−cysteine interaction could explain the NO-dependence of τ_4, but not τ_2, as observed by Yoo et al. [30] Those authors described a structural change in sGC that occurs on a timescale between τ_2 and τ_3 in order to account for the vastly different time scales of iron–histidyl bond cleavage. However, no explanation why τ_4, but not τ_2, depends on NO concentration was provided. An interaction between NO and a cysteine is likely to occur on this timescale and induce the observed structural transition. This conformational change could then influence the cleavage of the iron–histidyl bond, thereby accounting for the NO-dependence of τ_4.

Cary et al. [16] showed that small molecule sGC stimulators synergize with the 1-NO state of the enzyme. However, discovering precisely how NO and stimulators activate sGC to maximal activity is of great interest and directly relevant to the therapeutic action of these molecules. Despite a number of studies that seek to identify or narrow down the site of stimulator binding [71–79], the mechanism by which sGC activity is increased is still unknown. A recent study by Wales et al. [80] localizes the stimulator binding site between the N- and C- terminal subdomains of the β1 H−NOX domain, clarifying the specificity of these stimulators to sGCs. Further studies focused on the interaction between stimulators and sGC residues will parse out the necessary steps for stimulator activation and their synergy with NO.

3.4. sGC activation in cells

sGC activation should occur on similar timescales with the same ligand dependence, whether measured with purified enzyme or in cells. If this is not the case, it could signify that additional cofactors or binding partners are missing with studies conducted with purified enzyme. Measuring sGC activity directly in cells is challenging experimentally, and yet significant progress has been made toward this goal. Bellamy et al. [81] constructed an apparatus to reliably quench rat cerebellar cell suspensions on millisecond timescales. No lag in the synthesis of cGMP was detected, even at 20 ms after addition of NO, indicating that sGC is activated on sub-millisecond timescales at cellular concentrations of sGC. This is in agreement with the timescale of sGC activation as measured with purified enzyme [29].

Concerning the ligation state of sGC, there is currently no accurate method to measure the ligation state of heme cofactors *in vivo*. However, the assumption that sGC in cells has NO bound to the β H-NOX domain is based on two different sets of experiments. The first is that free NO has been measured by a variety of techniques, including fluorescent probes, NO biosensors, and several other methods. These studies indicate that the physiological signaling concentrations of NO are between 100 pM and 5 nM [82–86]. This is 100 to 1000-

fold higher than the dissociation constant for NO bound to the H−NOX domain of sGC (K_d < 1.2 × 10^{-12} M) [29]. Based on these values, it seems likely that the resting ligation state of sGC in cells is 5c Fe^{2+}−NO. The second set of experiments examined the effect of adding a small molecule sGC stimulator to human umbilical vein endothelial cells [70]. Without the addition of excess NO, YC-1 was able to stimulate sGC activity. As work with purified enzyme shows YC-1 has very little effect on 5c His−Fe^{2+} sGC, this implies there is a ligand' bound to the heme cofactor of sGC in cells.

As discussed, measuring the ligation state of sGC in cells has been a formidable challenge. From work with purified enzyme, NO dissociates slowly from the heme, even in the presence of ATP and GTP [16]. However, either with purified enzyme or experiments done in cells, sGC activity quickly decreases once NO is removed [16,68,84,86]. Roy et al. measured the EC_{50} of sGC in rat platelets to be 11 ± 1 nM, with a Hill coefficient of 1.2 ± 0.1, and the authors concluded that sGC possesses one binding site for NO in this concentration range (approximately 1 nM-200 nM NO) [84]. One interpretation from these data is that the one binding site measured was for the heme. However given that the K_d of the H-NOX domain for NO is four orders of magnitude below the EC_{50} [29] and the Hill coefficient for NO activating purified sGC is 2.1, [67] another interpretation of these data is that sGC in cells already has NO at the heme and the one binding site measured is the second site cysteine interaction.

Using the recently developed fluorescent cGMP biosensor δ-FlincG, Batchelor et al. [85] measured sGC activation at very low concentrations of NO, in the picomolar range. They developed a model that accounts for both sGC activation and the phosphodiesterase activity that degrades the cGMP signal. An increase in activity at such a low NO concentration is unusual, but the authors argue that the efficiency of signal transduction (defined as the turnover of enzyme per molecule of NO) is highest under these conditions. These experiments demonstrate that sGC can respond to exquisitely low amounts of NO, much lower than previously thought. The EC_{50} for NO in these studies depended on the relative concentrations of sGC and phosphodiesterase, however it is likely between 1 and 10 nM, in agreement with other studies done in platelets and astrocytes [87,88]. Thus, studies conducted in cells are consistent with work with purified enzyme and demonstrate that sGC activates on sub-second timescales, the ligation state of the H-NOX is likely 5c Fe^{2+}−NO, and sGC can respond to low amounts of NO.

4. Deactivation of soluble guanylate cyclase

4.1. Physiological deactivation of sGC

sGC deactivation is rapid following the removal of free, excess NO, both in cells and with purified enzyme [81,89]. To understand deactivation, the physiological concentrations of NO and sGC in cells must be considered. A recent estimate of sGC concentration in cells is 2 μM, deduced from cGMP formation in platelets using the kinetic parameters of isolated sGC [85]. Additionally, by deleting one isoform of the α-subunit of heterodimeric sGC and measuring the vascular response in both control and knockout mice, one study found that fewer copies of sGC can still elicit a full physiological response [90]. Thus, there is general agreement that sGC is present in excess relative to NO in cells.

As mentioned above, the ligation state of sGC in cells is assumed to be 5c Fe^{2+}−NO. This hypothesis stands in apparent contrast to the measured intracellular abundances of sGC (~ 2 μM) and NO (~ 1 nM); however, it should be noted that measurements of NO in cells is likely an underestimation as these data come from measurements made on free NO and thus sGC-bound NO is not accounted for in these estimations. Thus, since the measured concentration of free NO is higher than the dissociation constant of NO from the sGC heme ($K_d < 1.2 \times 10^{-12}$M) [29], we assume that all sGC in cells will have NO bound. Additionally, the half-life of most human proteins is on the order of hours, so even if not every sGC heterodimer is bound by NO immediately post translation, the majority of the population will exist long enough to bind to NO [91]. Consequently, all sGC in cells would be in the low-activity, 1-NO state (Fig. 8, middle). When the local concentration of free NO increases to nanomolar concentrations, NO will interact with the second binding site, and a small fraction of sGC will be converted to the fully active state. The estimation of nanomolar concentrations as the apparent K_d of the second site is deduced from the concentration of NO necessary to fully activate both purified sGC [54] and sGC in cells [84]. In this model, deactivation of this fraction is straightforward: as the concentration of NO decreases below 1 nM within a cell, the dissociation constant for the second site will favor NO release, returning sGC to the 1-NO state.

sGC stimulators were initially characterized as NO-independent, heme-dependent modulators of sGC activity. Indeed, in cell studies, stimulators increase sGC activity in the absence of excess NO. However, with purified enzyme, ligand binding to the heme is required to increase sGC activity, although the ligand can be either NO or CO. These differences can be reconciled by returning to the three-activity model. In cells, where the ligation state of the heme is assumed to be 5c Fe^{2+}−NO, the exogenous stimulator alone can render sGC fully active without the addition of additional NO. This model was further supported by cell studies where human umbilical vein endothelial cells (HUVECS) were pre-treated for 2 h with a nitric oxide synthase inhibitor N^{ω}-nitro-L-arginine methyl ester, essentially removing NO from the cells. Upon addition of YC-1, it was found that sGC activity in cells, as measured by cGMP production, was severely decreased [70], suggesting that a heme ligand is also necessary to activate sGC with YC-1. Deactivation proceeds once the stimulator concentration decreases below stimulator's K_d for sGC.

4.2. Pathophysiological deactivation of sGC

Low sGC activity has been implicated in several pathologies, including cardiopulmonary disease, hypertension, asthma, and neurodegeneration [12,92,93]. In particular, several studies have shown that prolonged oxidative stress deactivates sGC and renders it less responsive to NO. Currently, two different mechanisms have been hypothesized to explain these effects. First, direct oxidation of cysteine thiols to *S*-nitrosothiols could decrease sensitivity to NO by obscuring the putative secondary binding site, thereby preventing a necessary conformational change or decreasing substrate binding [94]. Second, oxidation of the ferrous heme could yield ferric- and subsequently apo-sGC [95]. The discussion here will focus on the molecular details by which sGC deactivates in these pathologies.

Sayed et al. [96] evaluated the extent of cysteine S-nitrosation of sGC in cells when exposed to excess NO. The authors treated smooth muscle cells, cells from rat aorta, and HUVECs to varying forms of NO, including *S*-nitrosocysteine, vascular endothelial growth factor, and acetylcholine. The authors found that sGC was *S*-nitrosated and desensitized to NO. While it is known that sGC requires reduced cysteines to function, this study was the first to show that *S*-nitrosation directly leads to desensitized sGC. In a follow-up study, neonatal cardiomyocytes were exposed to NO to carry out the *S*-nitrosations in a biologically-relevant environment [97]. After examining the enriched peptides by mass spectrometry, nine new sites of *S*-nitrosation on sGC were identified. While the majority of these sites were localized to the CAT domain, two were identified in the active site pocket, suggesting that decreased substrate binding may cause desensitization.

Heme oxidation can also affect sGC activity. A recent paper by Surmeli et al. [98] provided the first biochemical data showing that ferric sGC loses heme more readily than ferrous sGC, confirming a longstanding hypothesis [99]. Apo-sGC is then quickly degraded by cells [100]. One study has sought to unify these two modes of deactivation, where ferric-nitrosyl heme of sGC may undergo reductive elimination to generate a ferrous heme and an *S*-nitrosated cysteine [101]. The authors show that exogenous thiols prevent this S-nitrosation event from occurring with ferric-nitrosyl sGC, restoring sGC sensitivity to NO. However additional studies are necessary to confirm this hypothesis.

5. Conclusion

The eukaryotic nitric oxide receptor sGC plays a pivotal role in eukaryotic gas signaling and is essential for many physiological processes that affect human health. The biochemical activation and deactivation of sGC has been challenging to understand, partly because of the difficulty in generating large quantities of homogeneous protein, but more so due to the complexity of the activation mechanism of the enzyme. To date, the best supported model of sGC activation and deactivation is outlined in Fig. 8. In this three-activity model, the first molecule of NO binds on the distal side of the heme in the H-NOX domain, resulting in a partially activated enzyme. As the concentration of NO increases to nanomolar levels, NO interacts with the second site on sGC to fully activate the enzyme. As this concentration decreases, NO dissociates from the second site, and returns the enzyme to partial activity.

Moving forward, biochemical investigations centered on sGC should be validated on the full-length enzyme whenever possible to ensure catalytic competence. While truncations of sGC are easier to obtain, the full-length heterodimer is the only known form to exhibit the intricate activation sequence. Advances in structural biology techniques in the past few years —in particular cryo-electron microscopy—could provide a high-resolution quaternary structure of sGC and aid in answering some of the most difficult outstanding biochemical questions. Until that time, great care must be exercised in designing experiments to gain further understanding of this complex signaling enzyme.

Acknowledgements

B.G.H. and M.A.M. would like to thank the other members of the Marletta lab for fruitful discussions and critical review of this manuscript. B.G.H. was supported in part by a NIH Chemistry-Biology Interface Institutional Training Grant (T32 GM066698).

References

[1]. Furchgott RF, Zawadzki JV, The obligatory role of endothelial cells in the relaxation of arterial smooth muscle by acetylcholine, Nature 288 (1980) 373–376. [PubMed: 6253831]

[2]. Palmer RM, Ferrige AG, Moncada S, Nitric oxide release accounts for the biological activity of endothelium-derived relaxing factor, Nature 327 (1987) 524–526. [PubMed: 3495737]

[3]. Ignarro LJ, Byrns RE, Buga GM, Wood KS, Endothelium-derived relaxing factor from pulmonary artery and vein possesses pharmacologic and chemical properties identical to those of nitric oxide radical, Circ. Res 61 (1987) 866–879. [PubMed: 2890446]

[4]. Marletta MA, Yoon PS, Iyengar R, Leaf CD, Wishnok JS, Macrophage oxidation of L-arginine to nitrite and nitrate: nitric oxide is an intermediate, Biochemistry 27 (1988) 8706–8711. [PubMed: 3242600]

[5]. Knowles RG, Palacios M, Palmer RM, Moncada S, Formation of nitric oxide from L-arginine in the central nervous system: a transduction mechanism for stimulation of the soluble guanylate cyclase, Proc. Natl. Acad. Sci. U. S. A 86 (1989) 5159–5162. [PubMed: 2567995]

[6]. Moncada S, Palmer RM, Higgs EA, Nitric oxide: physiology, pathophysiology, and pharmacology, Pharmacol. Rev 43 (1991) 109–142. [PubMed: 1852778]

[7]. Steinert JR, Chernova T, Forsythe ID, Nitric oxide signaling in brain function, dysfunction, and dementia, Neuroscientist 16 (2010) 435–452. [PubMed: 20817920]

[8]. Gibson NJ, Nighorn A, Expression of nitric oxide synthase and soluble guanylyl cyclase in the developing olfactory system of Manduca sexta, J. Comp. Neurol 422 (2000) 191–205. [PubMed: 10842227]

[9]. Hervé D, et al., Loss of α1£1 soluble guanylate cyclase, the major nitric oxide receptor, leads to moyamoya and achalasia, Am. J. Hum. Genet 94 (2014) 385–394. [PubMed: 24581742]

[10]. Wen H-C, et al., Elevation of soluble guanylate cyclase suppresses proliferation and survival of human breast cancer cells, PLoS One 10 (2015) e0125518. [PubMed: 25928539]

[11]. Arnold WP, Mittal CK, Katsuki S, Murad F, Nitric oxide activates guanylate cyclase and increases guanosine 3':5'-cyclic monophosphate levels in various tissue preparations, Proc. Natl. Acad. Sci. U. S. A 74 (1977) 3203–3207. [PubMed: 20623]

[12]. Bredt DS, Endogenous nitric oxide synthesis: biological functions and pathophysiology, Free Radic. Res 31 (1999) 577–596. [PubMed: 10630682]

[13]. Friebe A, Koesling D, The function of NO−sensitive guanylyl cyclase: what we can learn from genetic mouse models, Nitric Oxide Biol. Chem 21 (2009) 149–156.

[14]. Ko FN, Wu CC, Kuo SC, Lee FY, Teng CM, YC-1, a novel activator of platelet guanylate cyclase, Blood 84 (1994) 4226–4233. [PubMed: 7527671]

[15]. Stasch J, Evgenov OV, Pharmacotherapy of Pulmonary Hypertension vol. 218, (2013).

[16]. Cary SPL, Winger JA, Marletta MA, Tonic and acute nitric oxide signaling through soluble guanylate cyclase is mediated by nonheme nitric oxide, ATP, and GTP, Proc. Natl. Acad. Sci. U. S. A 102 (2005) 13064–13069. [PubMed: 16131543]

[17]. Follmann M, et al., The chemistry and biology of soluble guanylate cyclase stimulators and activators, Angew. Chem. Int. Ed 52 (2013) 9442–9462.

[18]. Costell MH, et al., Comparison of soluble guanylate cyclase stimulators and activators in models of cardiovascular disease associated with oxidative stress, Front. Pharmacol 3 7 (2012) 1–14. [PubMed: 22291651]

[19]. Budworth J, Meillerais S, Charles I, Powell K, Tissue distribution of the human soluble guanylate cyclases, Biochem. Biophys. Res. Commun 263 (1999) 696–701. [PubMed: 10512742]

[20]. Zhao Y, Schelvis J, Babcock G, Marletta M, Identification of histidine 105 in the beta1 subunit of soluble guanylate cyclase as the heme proximal ligand, Biochemistry 37 (1998) 4502–4509. [PubMed: 9521770]

[21]. Derbyshire ER, Marletta MA, Structure and regulation of soluble guanylate cyclase, Annu. Rev. Biochem 81 (2012) 533–559. [PubMed: 22404633]

[22]. Montfort WR, Wales J, Weichsel A, Structure and activation of soluble guanylyl cyclase, the nitric oxide sensor, Antioxidants Redox Signal 0 (2016) 1–16.

[23]. Nioche P, et al., Femtomolar sensistivity of a NO sensor from Clostridium botulinum, Science 306 (2004) 1550–1554. [PubMed: 15472039]

[24]. Iyer L, Anantharaman V, Aravind L, Ancient conserved domains shared by animal soluble guanylyl cyclases and bacterial signaling proteins, BMC Genom 4 (2003) 5.

[25]. Karow DS, et al., Spectroscopic characterization of the soluble guanylate cyclaselike heme domains from Vibrio cholerae and Thermoanaerobacter tengcongensis, Biochemistry 43 (2004) 10203–10211. [PubMed: 15287748]

[26]. Ma X, Sayed N, Beuve A, van den Akker F, NO and CO differentially activate soluble guanylyl cyclase via a heme pivot-bend mechanism, EMBO J 26 (2007) 578–588. [PubMed: 17215864]

[27]. Martin F, et al., Structure of cinaciguat (BAY 58–2667) bound to Nostoc H−NOX domain reveals insights into heme-mimetic activation of the soluble guanylyl cyclase, J. Biol. Chem 285 (2010) 22651–22657. [PubMed: 20463019]

[28]. Rao M, Herzik MA, Iavarone AT, Marletta MA, Nitric oxide-induced conformational changes Govern H−NOX and histidine kinase interaction and regulation in Shewanella oneidensis, Biochemistry 56 (2017) 1274–1284. [PubMed: 28170222]

[29]. Zhao Y, Brandish P, Ballou D, Marletta MA, A Molecular basis for nitric oxide sensing by soluble guanylate cyclase, Proc. Natl. Acad. Sci. U. S. A 96 (1999) 14753–14758. [PubMed: 10611285]

[30]. Yoo B-K, Lamarre I, Martin J-L, Rappaport F, Negrerie M, Motion of proximal histidine and structural allosteric transition in soluble guanylate cyclase, Proc. Natl. Acad. Sci. U. S. A 112 (2015) E1697–E1704. [PubMed: 25831539]

[31]. Stone JR, Marletta MA, Soluble guanylate cyclase from bovine lung: activation with nitric oxide and carbon monoxide and spectral characterization of the ferrous and ferric states, Biochemistry 33 (1994) 5636–5640. [PubMed: 7910035]

[32]. Hunt AP, Lehnert N, Heme-nitrosyls: electronic structure implications for function in biology, Acc. Chem. Res (2015) 2117–2125, 10.1021/acs.accounts.5b00167. [PubMed: 26114618]

[33]. Herzik MA, Jonnalagadda R, Kuriyan J, Marletta MA, Structural insights into the role of iron-histidine bond cleavage in nitric oxide-induced activation of H-NOX gas sensor proteins, Proc. Natl. Acad. Sci. U. S. A 111 (2014) E4156–E4164. [PubMed: 25253889]

[34]. Baskaran P, Heckler EJ, van den Akker F, Beuve A, Identification of residues in the heme domain of soluble guanylyl cyclase that are important for basal and stimulated catalytic activity, PLoS One 6 (2011).

[35]. Baskaran P, Heckler EJ, Van Den Akker F, Beuve A, Aspartate 102 in the heme domain of soluble guanylyl cyclase has a key role in no activation, Biochemistry 50 (2011) 4291–4297. [PubMed: 21491881]

[36]. Henry JT, Crosson S, Ligand-binding PAS domains in a genomic, cellular, and structural context, Annu. Rev. Microbiol 65 (2011) 261–286. [PubMed: 21663441]

[37]. Möglich A, Ayers RA, Moffat K, Structure and signaling mechanism of per-ARNT-sim domains, Structure 17 (2009) 1282–1294. [PubMed: 19836329]

[38]. Ma X, Sayed N, Baskaran P, Beuve A, Van Den Akker F, PAS-mediated dimerization of soluble guanylyl cyclase revealed by signal transduction histidine kinase domain crystal structure, J. Biol 283 (2007) 1167–1178.

[39]. Zhao Y, Marletta MA, Localization of the heme binding region in soluble guanylate cyclase, Biochemistry 36 (1997) 15959–15964. [PubMed: 9398330]

[40]. Fritz B, et al., Molecular model of a soluble guanylyl cyclase fragment determined by small-angle X-ray scattering and chemical cross-linking, Biochemistry 52 (2013) 1568–1582. [PubMed: 23363317]

[41]. Sarkar A, et al., Heat shock protein 90 associates with the per-arnt-sim domain of heme-free soluble guanylate cyclase, J. Biol. Chem 290 (2015) 21615–21628. [PubMed: 26134567]

[42]. Purohit R, Weichsel A, Montfort WR, Crystal structure of the Alpha subunit PAS domain from soluble guanylyl cyclase, Protein Sci 22 (2013) 1439–1444. [PubMed: 23934793]

[43]. Ma X, Beuve A, van den Akker F, Crystal structure of the signaling helix coiled-coil domain of the beta1 subunit of the soluble guanylyl cyclase, BMC Struct. Biol 10 (2010) 2. [PubMed: 20105301]

[44]. Campbell MG, Underbakke ES, Potter CS, Carragher B, Marletta MA, Singleparticle EM reveals the higher-order domain architecture of soluble guanylate cyclase, Proc. Natl. Acad. Sci. U. S. A 111 (2014) 2960–2965. [PubMed: 24516165]

[45]. Underbakke ES, et al., Nitric oxide-induced conformational changes in soluble guanylate cyclase, Cell Struct 22 (2014) 1–10.

[46]. Linder JU, Class III adenylyl cyclases: molecular mechanisms of catalysis and regulation, Cell. Mol. Life Sci 63 (2006) 1736–1751. [PubMed: 16786220]

[47]. Winger JA, Derbyshire ER, Lamers MH, Marletta MA, Kuriyan J, The crystal structure of the catalytic domain of a eukaryotic guanylate cyclase, BMC Struct. Biol 8 (2008) 42. [PubMed: 18842118]

[48]. Allerston CK, von Delft F, Gileadi O, Crystal structures of the catalytic domain of human soluble guanylate cyclase, PLoS One 8 (2013) e57644. [PubMed: 23505436]

[49]. Seeger F, et al., Interfacial residues promote an optimal alignment of the catalytic center in human soluble guanylate cyclase: heterodimerization is required but not sufficient for activity, Biochemistry 53 (2014) 2153–2165. [PubMed: 24669844]

[50]. Derbyshire ER, Fernhoff NB, Deng S, Marletta MA, Nucleotide regulation of soluble guanylate cyclase substrate specificity, Biochemistry 48 (2009) 7519–7524. [PubMed: 19527054]

[51]. Surmeli NB, Muskens FM, Marletta MA, The influence of nitric oxide on soluble guanylate cyclase regulation by nucleotides, J. Biol. Chem 290 (2015) 15570–15580. [PubMed: 25907555]

[52]. Vercellino I, et al., Role of the nucleotidyl cyclase helical domain in catalytically active dimer formation, Proc. Natl. Acad. Sci. U. S. A 114 (2017) E9821–E9828, 10.1073/pnas.1712621114. [PubMed: 29087332]

[53]. Winger JA, Marletta MA, Expression and characterization of the catalytic domains of soluble guanylate cyclase: interaction with the heme domain, Biochemistry 44 (2005) 4083–4090. [PubMed: 15751985]

[54]. Stone JR, Marletta MA, Spectral and kinetic studies on the activation of soluble guanylate cyclase by nitric oxide, Biochemistry 35 (1996) 1093–1099. [PubMed: 8573563]

[55]. Martin E, Berka V, Tsai A-L, Murad F, Soluble guanylyl cyclase: the nitric oxide receptor, Methods Enzymol 396 (2005) 478–492. [PubMed: 16291255]

[56]. Martin E, Berka V, Sharina I, Tsai AL, Mechanism of binding of NO to soluble guanylyl cyclase: implication for the second NO binding to the heme proximal site, Biochemistry 51 (2012) 2737–2746. [PubMed: 22401134]

[57]. Makino R, et al., EPR characterization of axial bond in metal center of native and cobalt-substituted guanylate cyclase, J. Biol. Chem 274 (1999) 7714–7723. [PubMed: 10075661]

[58]. Martin E, Berka V, Bogatenkova E, Murad F, Tsai AL, Ligand selectivity of soluble guanylyl cyclase: effect of the hydrogen-bonding tyrosine in the distal heme pocket on binding of oxygen, nitric oxide, and carbon monoxide, J. Biol. Chem 281 (2006) 27836–27845. [PubMed: 16864588]

[59]. Dierks EA, et al., Demonstration of the role of scission of the proximal histidine-iron bond in the activation of soluble guanylyl cyclase through metalloporphyrin substitution studies, J. Am. Chem. Soc 119 (1997) 7316–7323.

[60]. Bellamy TC, Wood J, Garthwaite J, On the activation of soluble guanylyl cyclase by nitric oxide, Proc. Natl. Acad. Sci. U. S. A 99 (2002) 507–510. [PubMed: 11752394]

[61]. Ballou DP, Zhao Y, Brandish PE, Marletta MA, Revisiting the kinetics of nitric oxide (NO) binding to soluble guanylate cyclase: the simple NO−binding model is incorrect, Proc. Natl. Acad. Sci. U. S. A 99 (2002) 12097–12101. [PubMed: 12209005]

[62]. Lawson DM, Stevenson CE, Andrew CR, Eady RR, Unprecedented proximal binding of nitric oxide to heme: implications for guanylate cyclase, EMBO J 19 (2000) 5661–5671. [PubMed: 11060017]

[63]. Hespen CW, Bruegger JJ, Phillips-Piro CM, Marletta MA, Structural and functional evidence indicates selective oxygen signaling in Caldanaerobacter sub-terraneus H-NOX, ACS Chem. Biol 13 (2016) 1216–1221, 10.1021/acschembio.6b00431.

[64]. Negrerie M, Bouzhir L, Martin JL, Liebl U, Control of nitric oxide dynamics by guanylate cyclase in its activated state, J. Biol. Chem 276 (2001) 46815–46821. [PubMed: 11590135]

[65]. Yoo BK, Lamarre I, Martin JL, Negrerie M, Quaternary structure controls ligand dynamics in soluble guanylate cyclase, J. Biol. Chem 287 (2012) 6851–6859. [PubMed: 22223482]

[66]. Guo Y, et al., Regulation of nitric oxide signaling by formation of a distal receptor-ligand complex, Nat. Chem. Biol 13 (2017) 1216–1221, 10.1038/nchembio.2488. [PubMed: 28967923]

[67]. Bellamy TC, Griffiths C, Garthwaite J, Differential sensitivity of guanylyl cyclase and mitochondrial respiration to nitric oxide measured using clamped concentrations, J. Biol. Chem 277 (2002) 31801–31807. [PubMed: 12080082]

[68]. Russwurm M, Koesling D, NO activation of guanylyl cyclase, EMBO J 23 (2004) 4443–4450. [PubMed: 15510222]

[69]. Derbyshire ER, Marletta MA, Butyl isocyanide as a probe of the activation mechanism of soluble guanylate cyclase: investigating the role of non-heme nitricoxide, J. Biol. Chem 282 (2007) 35741–35748. [PubMed: 17916555]

[70]. Fernhoff NB, Derbyshire ER, Marletta MA, A nitric oxide/cysteine interaction mediates the activation of soluble guanylate cyclase, Proc. Natl. Acad. Sci. U. S. A 106 (2009) 21602–21607. [PubMed: 20007374]

[71]. Stasch JP, et al., NO−independent regulatory site on soluble guanylate cyclase, Nature 410 (2001) 212–215. [PubMed: 11242081]

[72]. Lamothe M, Chang FJ, Balashova N, Shirokov R, Beuve A, Functional characterization of nitric oxide and YC-1 activation of soluble guanylyl cyclase: structural implication for the YC-1 binding site? Biochemistry 43 (2004) 3039–3048. [PubMed: 15023055]

[73]. Martin E, Czarnecki K, Jayaraman V, Murad F, Kincaid J, Resonance Raman and infrared spectroscopic studies of high-output forms of human soluble guanylyl cyclase, J. Am. Chem. Soc 127 (2005) 4625–4631. [93] [PubMed: 15796527]

[74]. Yazawa S, Tsuchiya H, Hori H, Makino R, Functional characterization of two nucleotide-binding sites in soluble guanylate cyclase, J. Biol. Chem 281 (2006) 21763–21770. [PubMed: 16754683]

[75]. Hu X, et al., Allostery in recombinant soluble guanylyl cyclase from Manduca sexta, J. Biol. Chem 283 (2008) 20968–20977. [PubMed: 18515359]

[76]. Ibrahim M, Derbyshire ER, Marletta MA, Spiro TG, Probing soluble guanylate cyclase activation by CO and YC-1 using resonance Raman spectroscopy, Biochemistry 49 (2010) 3815–3823. [PubMed: 20353168]

[77]. Ibrahim M, Derbyshire ER, Soldatova AV, Marletta MA, Spiro TG, Soluble guanylate cyclase is activated differently by excess no and by YC-1: resonance Raman spectroscopic evidence, Biochemistry 49 (2010) 4864–4871. [PubMed: 20459051]

[78]. Yoo B-K, Lamarre I, Martin J-L, Negrerie M, Quaternary structure controls ligand dynamics in soluble guanylate cyclase, J. Biol. Chem 287 (2012) 6851–6859. [99] [PubMed: 22223482]

[79]. Purohit R, et al., YC-1 binding to the p subunit of soluble guanylyl cyclase overcomes allosteric inhibition by the a subunit, Biochemistry 53 (2014) 101–114. [PubMed: 24328155]

[80]. Wales JA, et al., Discovery of stimulator binding to a conserved pocket in the heme domain of soluble guanylyl cyclase, J. Biol. Chem 293 (2018) 1850–1864. [101] [PubMed: 29222330]

[81]. Bellamy TC, Garthwaite J, Sub-second kinetics of the nitric oxide receptor, soluble guanylyl cyclase, in intact cerebellar cells, J. Biol. Chem 276 (2001) 4287–4292. [PubMed: 11073946]

[82]. Hall CN, Garthwaite J, What is the real physiological NO concentration in vivo? Nitric Oxide Biol. Chem 21 (2009) 92–103.

[83]. Roy B, Halvey EJ, Garthwaite J, An enzyme-linked receptor mechanism for nitric oxide-activated guanylyl cyclase, J. Biol. Chem 283 (2008) 18841–18851. [PubMed: 18463095]

[84]. Roy B, Garthwaite J, Nitric oxide activation of guanylyl cyclase in cells revisited, Proc. Natl. Acad. Sci. U. S. A 103 (2006) 12185–12190. [PubMed: 16882726]

[85]. Batchelor AM, et al., Exquisite sensitivity to subsecond, picomolar nitric oxide transients conferred on cells by guanylyl cyclase-coupled receptors, Proc. Natl. Acad. Sci. U. S. A 107 (2010) 22060–22065. [PubMed: 21135206]

[86]. Wood KC, et al., Picomolar nitric oxide signals from central neurons recorded using ultrasensitive detector cells, J. Biol. Chem 286 (2011) 43172–43181. [PubMed: 22016390]

[87]. Mo E, Amin H, Bianco IH, Garthwaite J, Kinetics of a cellular nitric oxide/cGMP/phosphodiesterase-5 pathway, J. Biol. Chem 279 (2004) 26149–26158. [PubMed: 15075333]

[88]. Halvey EJ, Vernon J, Roy B, Garthwaite J, Mechanisms of activity-dependent plasticity in cellular nitric oxide-cGMP signaling, J. Biol. Chem 284 (2009) 25630–25641. [PubMed: 19605352]

[89]. Margulis A, Sitaramayya A, Rate of deactivation of nitric oxide-stimulated soluble guanylate cyclase: influence of nitric oxide scavengers and calcium, Biochemistry 39 (2000) 1034–1039. [PubMed: 10653648]

[90]. Mergia E, Friebe A, Dangel O, Russwurm M, Koesling D, Spare guanylyl cyclase NO receptors ensure high NO sensitivity in the vascular system, J. Clin. Invest 116 (2006) 1731–1737. [PubMed: 16614755]

[91]. Bojkowska K, et al., Measuring in vivo protein half-life, Chem. Biol 18 (2011) 805–815. [PubMed: 21700215]

[92]. Ritchie RH, Drummond GR, Sobey CG, De Silva TM, Kemp-Harper BK, The opposing roles of NO and oxidative stress in cardiovascular disease, Pharmacol. Res 116 (2016) 57–69. [PubMed: 27988384]

[93]. Ghosh A, et al., Soluble guanylate cyclase as an alternative target for broncho-dilator therapy in asthma, Proc. Natl. Acad. Sci. U. S. A 113 (2016) E2355–E2362. [PubMed: 27071111]

[94]. Beuve A, Thiol-based redox modulation of soluble guanylyl cyclase, the nitric oxide receptor, Antioxid. Redox Signal 26 (2017) 137–149. [PubMed: 26906466]

[95]. Stasch J-P, Pacher P, Evgenov OV, Soluble guanylate cyclase as an emerging therapeutic target in cardiopulmonary disease, Circulation 123 (2011) 2263–2273. [PubMed: 21606405]

[96]. Sayed N, Baskaran P, Ma X, van den Akker F, Beuve A, Desensitization of soluble guanylyl cyclase, the NO receptor, by S-nitrosylation, Proc. Natl. Acad. Sci. U. S. A 104 (2007) 12312–12317. [PubMed: 17636120]

[97]. Beuve A, et al., Identification of novel S-nitrosation sites in soluble guanylyl cyclase, the nitric oxide receptor, J. Proteomics 138 (2016) 40–47. [PubMed: 26917471]

[98]. Surmeli NB, Marletta MA, Insight into the rescue of oxidized soluble guanylate cyclase by the activator cinaciguat, Chembiochem 13 (2012) 977–981. [PubMed: 22474005]

[99]. Hobbs AJ, Soluble guanylate cyclase, emerging therapeutic targets, Emerg. Ther. Targets 4 (2000) 735–749.

[100]. Alexandre EC, et al., Soluble guanylyl cyclase (sGC) degradation and impairment of nitric oxide-mediated responses in urethra from obese mice: reversal by the sGC activator BAY 60–2770, J. Pharmacol. Exp. Ther 349 (2014) 2–9. [PubMed: 24421320]

[101]. Fernhoff NB, Derbyshire ER, Underbakke ES, Marletta MA, Heme-assisted S-nitrosation desensitizes ferric soluble guanylate cyclase to nitric oxide, J. Biol. Chem 287 (2012) 43053–43062. [PubMed: 23093402]

[102]. Kelly LA, et al., The Phyre2 portal web portal for protein modeling, prediction and analysis, Nature Protoc 10 (2015) 845–858. [PubMed: 25950237]

Box 1.

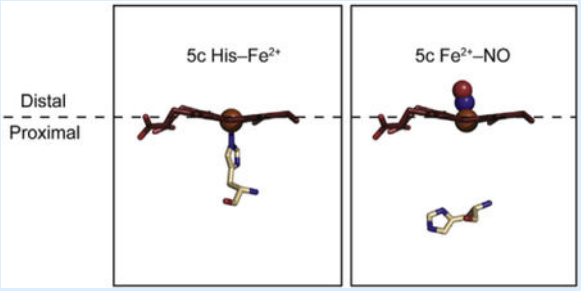

The heme cofactor in sGC has an inherent sidedness as defined by the presence of the coordinating histidine residue (H105 in *Homo sapiens* β1 sGC). The histidine binds to the ferrous iron of the heme cofactor from one side, termed the proximal side. The opposing side of the heme is referred to as the distal side. Upon binding of nitric oxide (NO) to the distal side of the heme, the strong o trans effect of NO induces rupture of the iron–histidyl bond, which is thought to be the first step in signal transduction. However, this cleavage event results in the opening of the proximal coordination site for an additional NO molecule to bind. To clarify the potential heme ligation states in sGC, the following naming convention will be used in this review: 4/5/6c (proximal ligand)−M^{n+}−(distal ligand), where 4/5/6c refers to the coordination number of the M^{n+} center. For example, unliganded ferrous sGC with the proximal histidine bound would be described as 5c His−Fe^{2+}, whereas a distal ferrous nitrosyl complex would be termed 5c Fe^{2+} −NO.

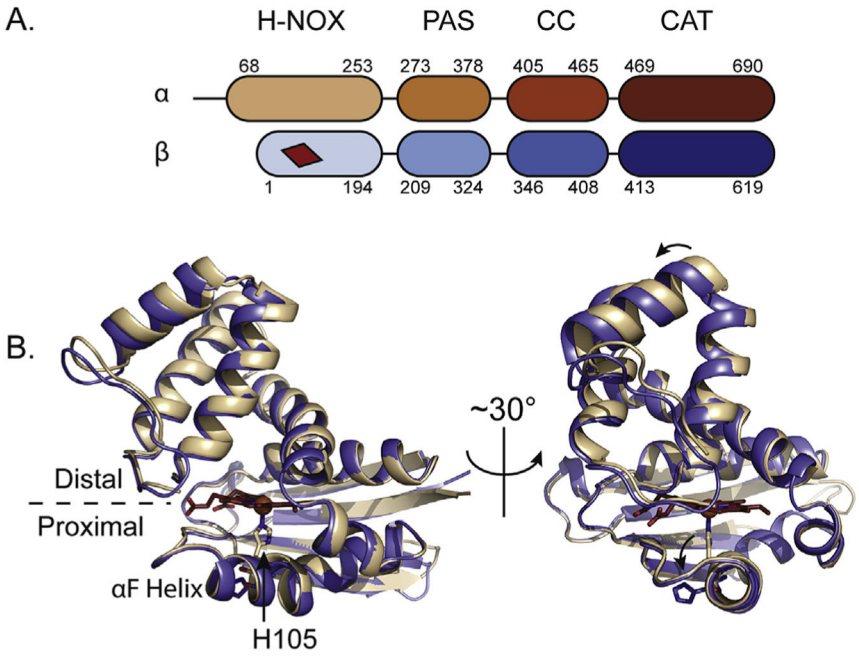

Fig. 1. Domain and subdomain organization of sGC

A) Schematic of soluble guanylate cyclase domains. The four domains of the *a* (in orange) and p (in blue) subunits are listed above the schematic representation: heme nitric oxide and oxygen binding domain (H-NOX), Per-Arnt-Sim domain (PAS), coiled-coil domain (CC), and the catalytic domain (CAT). The approximate numbering of the Human α1 and β1 domains is shown. The heme cofactor, shown as a red diamond, binds to β1 H105. B) Motions of heme nitric oxide and oxygen binding domains (H−NOX) upon nitric oxide binding. Overlay of the *Shewanella oneidensis* H-NOX domain in the Fe^{2+} (wheat, PDB ID: 4U99) and Fe^{2+}−NO (blue, PDB ID: 4U9B) states. Structures have been aligned by the proximal domains (residues 95–180). Displacement of the distal domain and rotation of the proximal histidine are noted with arrows. (For interpretation of the references to color in this figure legend, the reader is referred to the Web version of this article.)

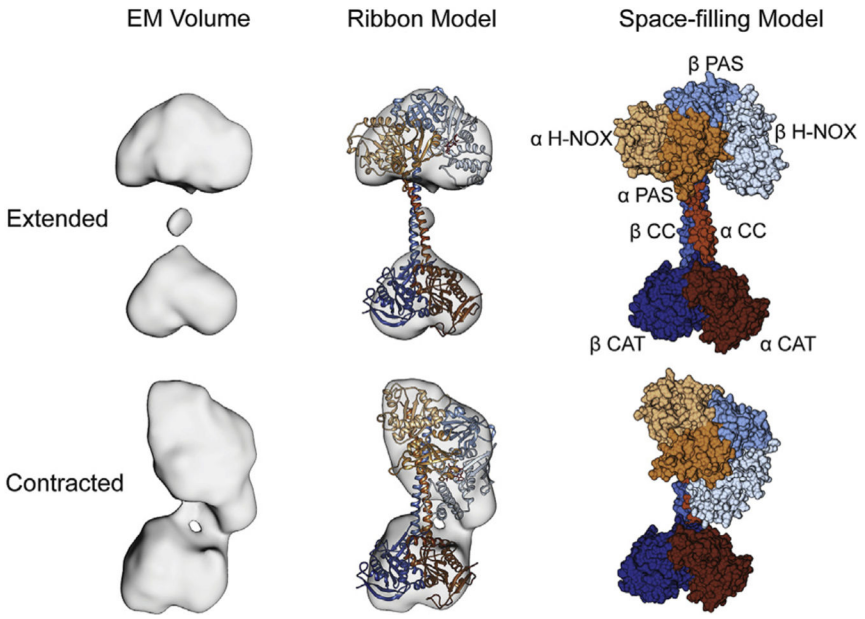

Fig. 2. Reconstructed full-length representation of sGC.

Using available crystal structures and single-particle electron microscopy data from Campbell et al. [40], a representation of the full-length structure of sGC was constructed. The subunits are colored as in Fig. 1A. Beginning with two representative EM volumes (left), the following crystal structures were fit into the densities: Human α1 and β1 sGC H-NOX domain homology models were derived from the bacterial H-NOX from *Nostoc sp* (PDB ID: 2O09); Human α1 and β1 PAS domain homology models were derived from eukaryotic PAS from *C. reinhardtii* (PDB ID: 4GJ4) and aligned using the *Nostoc punctiforme* PAS dimer (PDB ID: 2P04); Human α1 and β1 CC domain homology models and the human CAT structure (PDB ID: 4NI2) were aligned to the *Mycobacterium intracellulare* adenylate cyclase structure (PDB ID: 505l), chains C and D, and adjusted to fit within the volumes. These crystal structures have been fitted into the densities and are shown as ribbon diagrams (middle). The two extreme conformations of sGC are shown and labeled as “Extended” and “Contracted”. The space-filling model of both conformations is shown (right). All homology models were generated using thePhyre2 web portal [102].

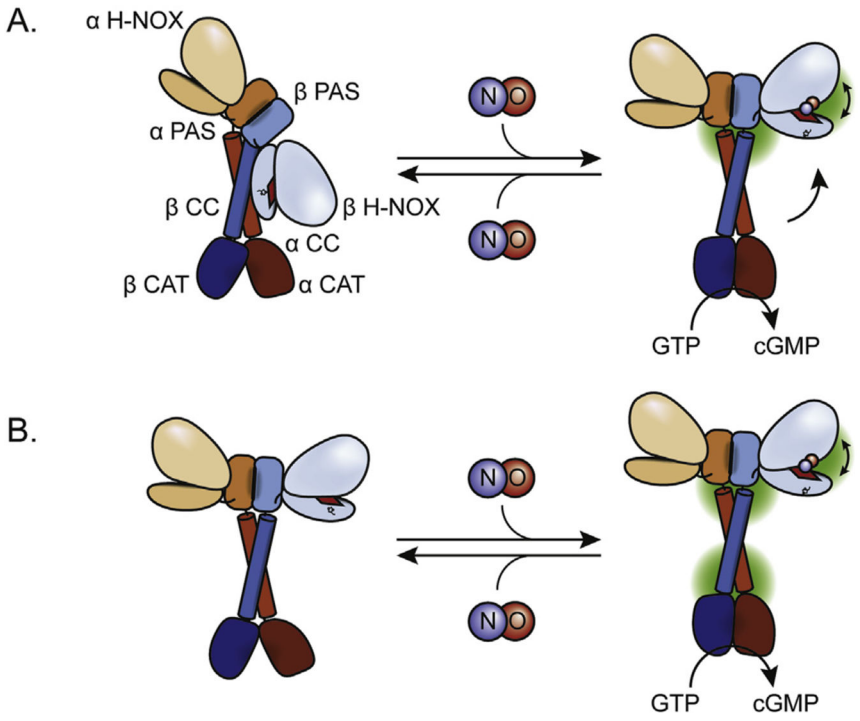

Fig. 3. Quaternary domain organization of sGC upon NO activation.

It is predicted that some spatial reorganization of the sGC domains occurs when NO activates the enzyme. A) Self-inhibition of sGC through contact of the β H-NOX domain to the α CAT domain, termed the contracted conformation. Upon NO binding, this contact would be released allowing a conformational change into the extended conformation which in full catalytic activity. B) When NO is not bound, the tertiary structure holds sGC in a non-active conformation while the quaternary structure is flexible (not depicted). Upon NO binding, structural rearrangements occur along the protein backbone, which results in full catalytic activity.

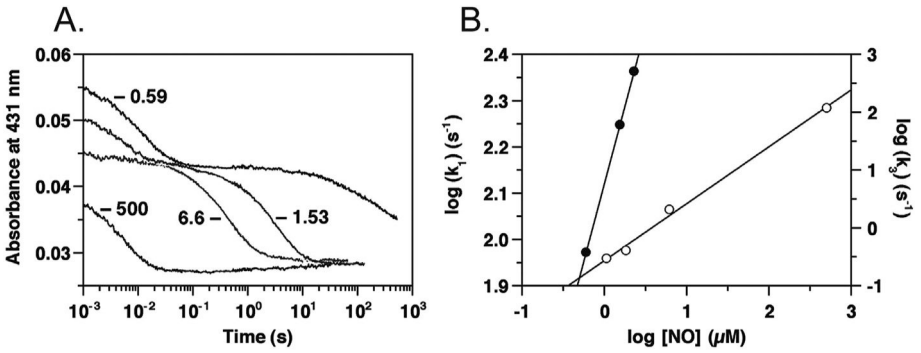

Fig. 4. Nitric oxide dependent spectral transitions in sGC.

Both the formation of the 6c ferrous nitrosyl complex and cleavage of the iron–histidyl bond are dependent on NO concentration. A) The absorbance at 431 nm, which corresponds to Soret maximum the 5c ferrous-histidine complex, decreases with time as sGC interacts with the indicated NO concentrations (in μM). B) Dependence of the slow and the fast rates extracted from A) on NO concentration. Adapted from Ref. [29].

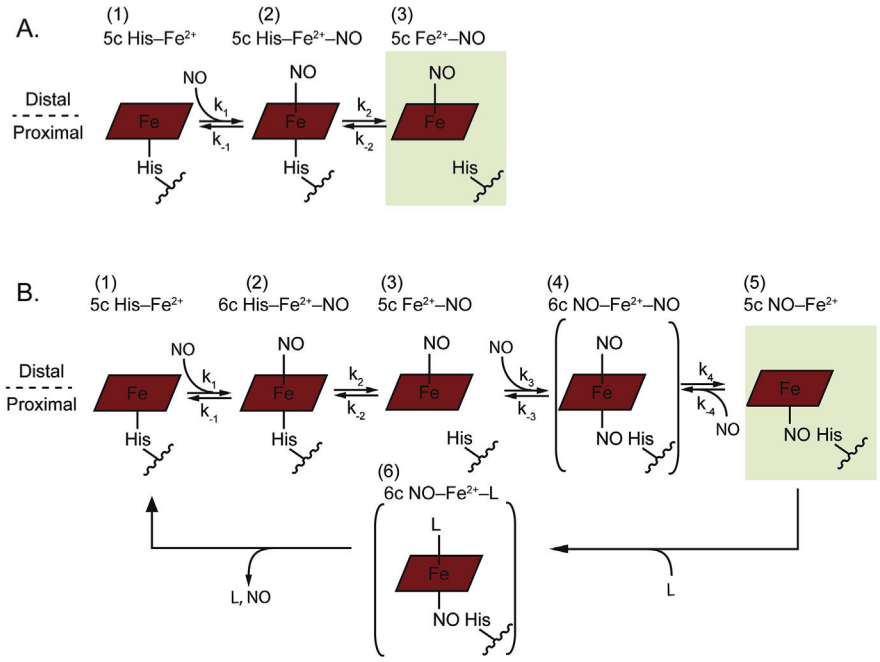

Fig. 5. Nitric oxide sidedness on the heme.

A depiction of the molecular steps of NO binding to and dissociation from the heme in sGC. A) NO binds to the distal side of the heme with an association rate of k_1 to form species (2). Rupture of the proximal histidine iron bond with the rate of k_2 yields species (3). Note that k_2 is dependent on NO concentration, as shown in Fig. 4. To reverse this process, the proximal histidine rebinds to the heme with a rate of k_{-2}, followed by the dissociation of NO from the distal side. B) For NO to bind on the proximal side of the heme, the distal 5c species must form first (as in A). Another molecule of NO binds to the proximal side of the heme with a rate of k_3 to form species (4), followed by the cleavage of the distal NO−Fe bond with a rate of k4 to yield species (5). The reverse of this process requires either excess NO (to undergo the microscopic reverse), or another ligand (L) to bind to the distal side of the heme. Figure adapted from Ref. [66].

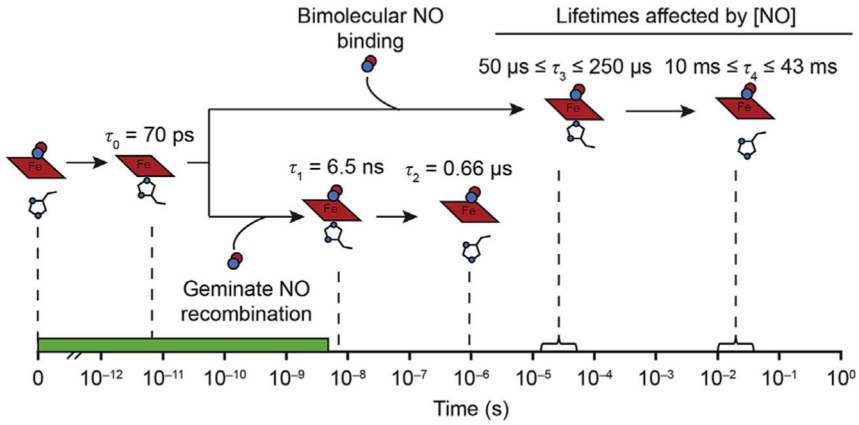

Fig. 6. Kinetics of sGC transitions in the heme pocket.

The fate of the 5c iron-histidine species formed after laser photolysis of NO is depicted. A 6 ns 532 nm laser pulse, indicated by the green bar, dissociates NO. The proximal histidine rebinds to the heme with a time constant of τ_0, measured in a separate experiment. There are two routes through which the 5c His−Fe^{2+} species can proceed. In the route occurring at faster timescales (bottom), geminate recombination of NO occurs with a lifetime of 6.5 ns, followed by cleavage of the iron–histidyl bond with a life time of 0.66 [is. τ_1 and τ_2 do not depend on NO concentration. In the route occurring at longer timescales (top), NO from the solution diffuses into the heme pocket in a bimolecular process and binds to the heme with lifetimes of 50 is ≤ τ_3 ≤ 250 is, followed by cleavage of the iron-histidyl bond with lifetimes of 10 ms ≤ τ_4 ≤ 43 ms (NO concentration between 20 iM and 200 iM). Both τ_3 and τ_4 are dependent on the NO concentration, consistent with the stopped-flow spectroscopy data in Fig. 4. Figure adapted from Ref. [30].

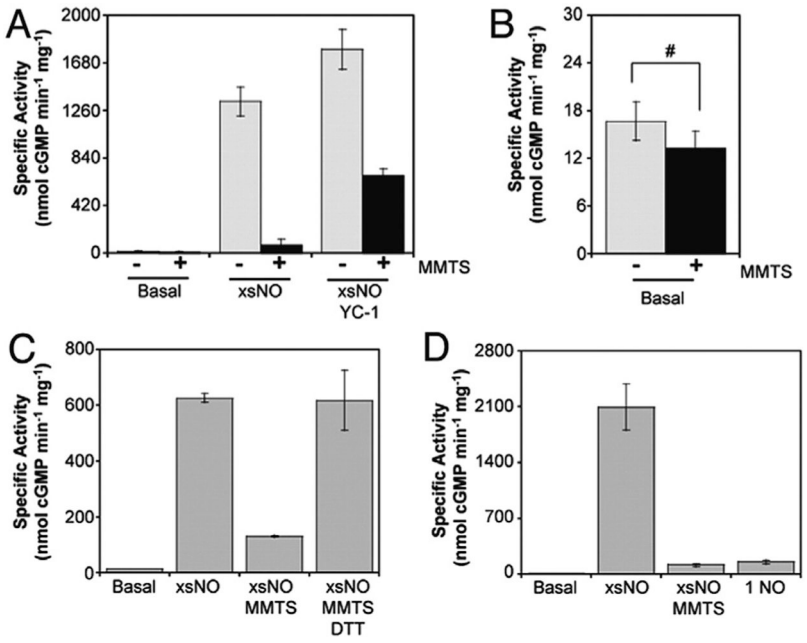

Fig. 7. Blocking of sGC cysteines prevents full enzyme activation.

A) Experimental data showing that MMTS-treated sGC will not fully activate with excess NO but will activate to a certain extent with NO and a stimulator. B) MMTS does not affect the basal activity level of sGC. C) Treatment of the MMTS-labeled enzyme with DTT reverses the inhibition. D) The activity of the MMTS-treated sGC is comparable to the activity of the 1-NO state. Figure reprinted from Ref. [70].

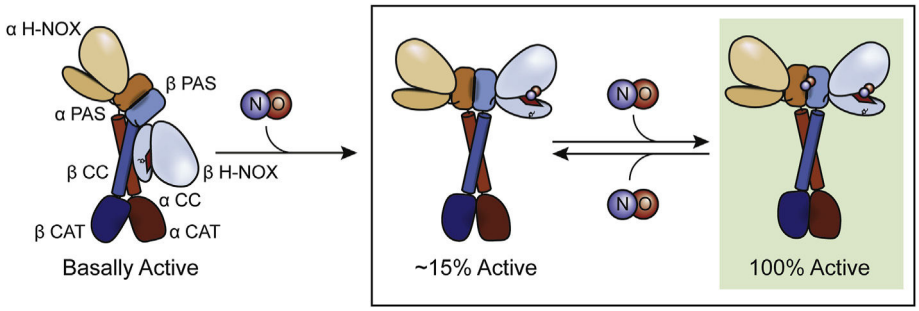

Fig. 8. sGC activation and deactivation in vivo.

A model that accounts for all available data of physiological sGC activation and deactivation is depicted. For ease of representation, the sGC state with basal activity is depicted in the conformation in which the β H-NOX contacts the α sGC CAT domain. It is not known how the overall quaternary structure of sGC changes upon NO binding. The first molecule of NO that sGC encounters will bind to the heme of the H-NOX domain with picomolar affinity and remain bound. Thus, the vast majority of sGC in cells will be in the ~15% active state (1-NO). With an increase in the NO cellular concentration, NO will interact with the second site, which has nanomolar affinity. The physiologically relevant sGC states are boxed. Although the location of the second site has not yet been located yet, it is depicted here in the PAS domains. The modulation between these two states accounts for the downstream effects of NO in cells, as well as the rapid activation and deactivation of sGC observed both with purified enzyme, in cells, and in tissues.